JOURNAL OF GEOPHYSICAL RESEARCH, VOL. 94, NO. B5, PAGES 5585–5602, MAY 10, 1989

Closure of the Africa-Eurasia-North America Plate Motion Circuit and Tectonics of the Gloria Fault

DONALD F. ARGUS, RICHARD G. GORDON, CHARLES DEMETS,[1] AND SETH STEIN

Department of Geological Sciences, Northwestern University, Evanston, Illinois

We examine the closure of the current plate motion circuit between the African, North American, and Eurasian plates to test whether these plates are rigid and whether the Gloria fault is an active transform fault. We also investigate the possible existence of microplates that have been previously proposed to lie along these plate boundaries, and compare the predicted direction of motion along the African-Eurasian plate boundary in the Mediterranean with the direction of slip observed in earthquakes. From marine geophysical data we obtain 13 transform fault azimuths and 40 3-m.y.-average spreading rates, 34 of which are determined from comparison of synthetic magnetic anomaly profiles to ~140 observed profiles. Slip vectors from 32 earthquake focal mechanisms further describe plate motion. Detailed magnetic surveys north of Iceland provide 11 rates in a region where prior plate motion models had few data. Magnetic profiles north of the Azores triple junction record a rate of 24 mm/yr, 4 mm/yr slower than used by prior models. Gloria and Sea Beam surveys accurately measure the azimuths of seven transform faults; our plate motion model fits six of the seven within 2°. Two transform faults surveyed by Gloria side scan sonar lie near FAMOUS area transform faults A and B and give azimuths 13° clockwise of them. Because recent studies show that short-offset transforms, such as transforms A and B, are in many places oblique to the direction of plate motion, we exclude azimuths from transforms with less than 35-km offset. The best fitting and closure-enforced vectors fit the data well, except for a small systematic misfit to the slip vectors: On right-lateral slipping transforms, slip vectors tend to be a few degrees clockwise of plate motion and mapped fault azimuths, whereas on left-lateral slipping transforms, slip vectors tend to be a few degrees counterclockwise of plate motion and mapped fault azimuths. We search the long Eurasia-North America boundary for evidence of an additional plate, but find no systematic misfits to the data. In particular, if a Spitsbergen plate exists and moves relative to Eurasia, its motion is less than 3 mm/yr. An Africa-Eurasia Euler vector determined by adding the Eurasia-North America and Africa-North America Euler vectors is consistent with the Gloria fault trend and with slip vectors from eastern Azores-Gibraltar Ridge focal mechanisms. A small circle, centered at the Africa-Eurasia closure-enforced pole, fits the trace of the Gloria fault. The model in which closure was enforced predicts ~4 mm/yr slip across the Azores-Gibraltar Ridge, and west-northwest convergence near Gibraltar, ~45° more oblique than suggested by a recent model based on compressive axes of focal mechanisms. Moreover, our model predicts directions of plate motion that agree well with northwest trending slip vectors from thrust earthquakes between Gibraltar and Sicily. Because closure-enforced vectors fit the data nearly as well as the best fitting vectors, we conclude that the data are consistent with a rigid plate model and with the Gloria fault being a transform fault.

INTRODUCTION

In this paper we present results of a study of the current motions of the African, Eurasian, and North American plates. We focus on several related questions: Do any obscure plate boundaries intersect the conventionally defined Eurasia-North America, Africa-North America, and Africa-Eurasia plate boundaries? In particular, is there a distinct Spitsbergen microplate that moves relative to Eurasia, as proposed by *Savostin and Karasik* [1981]? Are short- or long-offset transform faults better indicators of the direction of motion between the African and North American plates? Is the current motion between the African and Eurasian plates consistent with the Gloria fault (Figures 1 and 2) [*Laughton et al.*, 1972] being a true transform fault, and with observed directions of slip in the Mediterranean? Are different types of Arctic and North Atlantic plate motion data mutually consistent? Last, how well do these three plates obey the assumption of plate rigidity, i.e., is there any measurable nonclosure of this plate motion circuit that could be attributed to intraplate deformation? In the rest of this introduction we discuss the motivation and background for these problems.

The first problem we treat is the current motion between the Eurasian and North American plates, and whether there is resolvable motion of a Spitsbergen microplate. In part from high seismicity near the Svalbard Archipelago, *Savostin and Karasik* [1981] proposed that a Spitsbergen microplate lies southeast of the Arctic Ridge (Figure 1). However, *Bungum et al.* [1982] attributed the same seismicity to insignificant motion caused by the current stress field along old zones of weakness. As discussed below, we found no support for the existence of any microplate along the oceanic part of the Eurasia-North America boundary.

The second problem we investigate is the direction of motion between the African and North American plates. In studies of current global plate motions, *Minster et al.* [1974] and *Chase* [1978] used the trends of the long-

[1]Now at Naval Research Laboratory, Washington, D.C.

Paper number 88JB03988.
0148-0227/89/88JB-03988$05.00

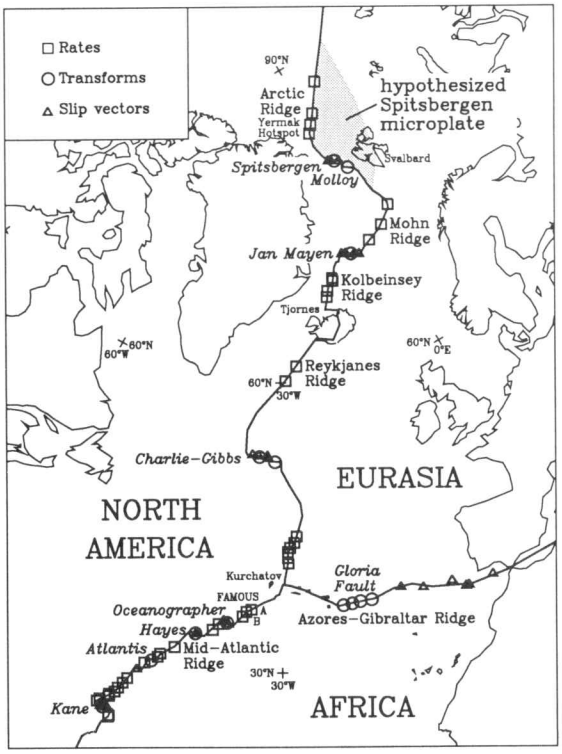

Fig. 1. Plate geometry and data locations. Every transform fault is labeled in italics. Transforms omitted from the data set (such as transforms A and B) are labeled in smaller letters. Good data extend well north of Iceland, a region that was poorly sampled in prior plate motion studies. The location of a hypothetical Spitsbergen microplate is shaded. Equal-area projection.

offset Oceanographer (S75°E) and Atlantis (S82°E) transforms (Figure 1) to estimate the direction of Africa-North America motion. A detailed study of the FAMOUS region (Figure 1), north of the Oceanographer, mapped the short-offset (20 km) transforms A and B, with trends (~N90°E) 15° discordant from the Oceanographer [*Macdonald and Luyendyk*, 1977]. Later, *Minster and Jordan* [1978] attributed the difference between the azimuths of the long-offset transforms and transforms A and B to a post-5 Ma change in direction of plate motion. They thus deleted the Oceanographer and Atlantis transforms from their plate motion data set, and replaced them with transforms A and B. However, they found in their global model that the trends of transforms A and B were systematically misfit by 5–10°, which they attributed to the forced closure about the Azores Triple Junction. Here we review the recent evidence that suggests that short-offset transforms are unreliable recorders of the direction of plate motion, and we determine Africa-North America motion without using the trends of any short-offset transform faults. The difference in trends between short- and long-offset transform faults has important implications for the third, and key, problem we consider here: the motion and tectonics along the Africa-Eurasia boundary.

The Mid-Atlantic Ridge, which is demarcated by its morphology, seismicity, and magnetic anomalies, is more sharply defined than the African-Eurasian plate boundary, which trends east-west and extends from the Azores Triple Junction, along the morphological Azores-Gibraltar Ridge, into the Mediterranean Sea (Figure 1). Moreover, while the rate and direction of motion along the Mid-

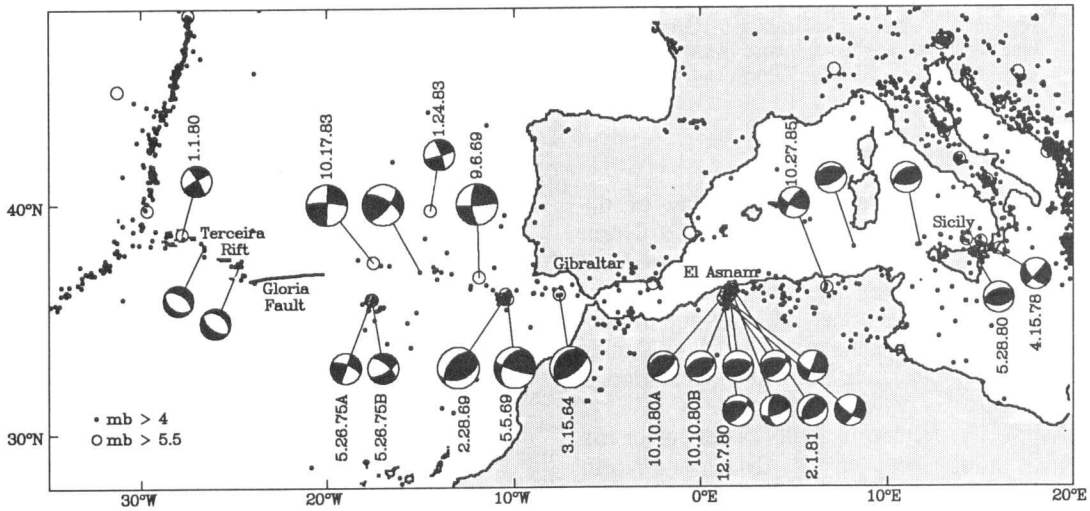

Fig. 2. Map showing earthquakes shallower than 100-km depth (reported in the Earthquake Data File of the National Geophysical Data Center) between 1964 and 1987 along the Eurasia-Africa plate boundary. Equal-area projections of the lower hemisphere of the focal sphere are plotted for the fault plane solutions of 26 large events where darkened quadrants correspond to compressional first motions. The six fault plane solutions plotted larger are used in the inversion; these lie within a narrow (~50 km wide) band of seismicity, extending from the east end of the Gloria fault to Gibraltar, which we take to be the plate boundary. Fault plane solutions lying off the boundary, such as the May 26, 1975, event (~200 km south of the seismicity band), were omitted in the inversion. Fault plane solutions west of Gibraltar are from *Grimison and Chen* [1986, 1988]; those east of Gibraltar are from the Harvard CMT solutions. No focal mechanisms from deep events are shown. Three events have surface wave magnitudes exceeding 7: the February 28, 1969, May 26, 1975, and October 10, 1980, earthquakes. Dates are given for fault plane solutions with body wave magnitudes exceeding 5.5.

Atlantic Ridge can be found from many magnetic profiles, the trends of prominent, well-mapped transform faults, and the focal mechanisms of earthquakes along them, the motion along the Africa-Eurasia boundary is poorly described. We focus on the western, oceanic segment along the Azores-Gibraltar Ridge, but will later examine how well the plate motion model determined from Atlantic data fits the orientations of slip vectors in the Mediterranean.

Motion across the Azores-Gibraltar Ridge is slow and includes northwest-southeast contraction in the east, east-west right-lateral strike slip near its center, and northeast-southwest extension along the Terceira rift in the west (Figure 2) [*McKenzie*, 1972; *Chase*, 1978; *Minster and Jordan*, 1978]. Near the Terceira rift, magnetic lineations that parallel the rift [*Searle*, 1980] and normal-faulting earthquake mechanisms [*Grimison and Chen*, 1986] suggest that it is spreading northeast. Along the eastern Azores-Gibraltar Ridge, thrust and strike-slip mechanisms, complex bathymetry dominated by large seamounts, diffuse seismicity with large earthquakes (three events with M_S between 7 and 8, three events with M_S exceeding 8 [*Grimison and Chen*, 1986]), and the absence of a Benioff zone suggest the ridge is a complex region of northwest directed ocean-ocean convergence. The Gloria fault, which extends from the east end of the Terceira rift (20°W), to the west end of the ocean-ocean convergent boundary, is a 400-km-long lineament recognized from long-range side scan sonar (Gloria) [*Laughton et al.*, 1972], and is thought to be a right-lateral strike-slip fault (Figure 2).

If the Gloria fault is a true transform fault, it is in an unusual tectonic setting. Nearly all oceanic transform faults offset spreading ridges, whereas the Gloria fault offsets a probable spreading ridge from a region of ocean-ocean convergence. *Laughton et al.* [1972], *Laughton and Whitmarsh* [1974], and *Searle* [1979] have argued that the Gloria fault is an active transform fault dividing the African and Eurasian plates. Evidence favoring the transform fault hypothesis includes the great length and straightness of the fault. The sharpness and narrowness of the Gloria reflections suggest a fresh, unsedimented scarp. The only other submarine tectonic features with comparable narrowness, straightness, and continuity are transform faults offsetting ridges. The Gloria fault divides regions of differing magnetic and bathymetric trends and differing crustal ages, which suggest large displacement along the fault [*Laughton and Whitmarsh*, 1974].

On the other hand, early models of African-Eurasian plate motion [*Morgan*, 1968; *McKenzie*, 1972; *Minster et al.*, 1974] disagree with the azimuth of the Gloria fault. Although *Minster and Jordan's* [1978] model RM2 fits the Gloria fault azimuth well, it does so at the cost of a poor fit to data along the Africa-North America boundary. *Grimison and Chen* [1986] concluded that the Azores-Gibraltar boundary is nowhere a transform fault because its associated earthquakes and bathymetric expression, including the Gloria fault, lie outside the small circle plate boundary they predict from RM2. They further conclude that, aside from the Terceira rift, all significant oceanic earthquakes along the Azores-Gibraltar plate boundary are part of a diffuse zone of ocean-ocean convergence. In their model the discrete Gloria fault cannot be a transform fault.

The fourth problem we treat, closely related to the second and third, is the question of plate circuit closure and its implications for rates of intraplate deformation. *Minster and Jordan* [1978] examined the closure of the Africa-Eurasia-North America plate circuit, and found that the best fitting Euler vectors describing the motion across each plate boundary were individually well constrained and internally consistent, but failed closure. *DeMets et al.* [1985] used a much larger and more recent data set and also found significant nonclosure. The nonclosure found in these prior studies might have stemmed from poor data along the Azores-Gibraltar Ridge (i.e., the Gloria fault may not be a true transform fault), poor data along the Mid-Atlantic Ridge, or from plate nonrigidity.

We began the detailed analysis of plate motion data presented here in part because our preliminary analysis [*DeMets et al.*, 1985] suggested significant nonclosure of this plate motion circuit. We expected to be able to show either that deformation of one of these plates is rapid enough to be measurable with plate motion data or that the Gloria fault could not be an active transform fault. To our surprise, however, we found that careful scrutiny of the plate motion data, especially spreading rates, leads to the opposite conclusion: that the data are consistent with a rigid plate model in which the Gloria fault is an active transform fault. Our new plate motion model also predicts directions of motion that are consistent with orientations of slip vectors from earthquakes in the Mediterranean region between Gibraltar and Sicily. We conclude that the nonclosure found before was caused by limitations of data along the Arctic and Mid-Atlantic ridges. In the following section we will discuss the data and results, first for each plate pair taken separately, and then for all three plates taken together. Details of our methods are given in the appendix.

BEST FITS TO INDIVIDUAL PLATE PAIRS

Eurasia-North America Motion

The present azimuthal data along the Eurasia-North America plate boundary are more numerous and accurate than those available to prior plate motion studies (Table 1). New maps showing the trends of the Jan Mayen and Spitsbergen transforms [*Perry et al.*, 1978], along with the accurate azimuths of the Gloria-surveyed northern and southern Charlie-Gibbs transforms [*Searle*, 1981], give the direction of Eurasian-North American motion and restrict the Euler pole to a narrow region elongated orthogonal to these transforms (Figures 1, 3, and 4, Table 2). Fourteen strike-slip mechanisms also help constrain the direction of motion (Table 1).

Each rate along the Eurasian-North American boundary is an average of rates from 2–15 profiles; they are the most accurate rates in this three-plate system. Prior plate motion models [*Chase*, 1978; *Minster and Jordan*, 1978] used few rates north of Iceland. We filled this spreading rate gap using many closely spaced aeromagnetic profiles across the Arctic (60 profiles), Mohn (40 profiles), and Kolbeinsey (60 profiles) ridges collected by

TABLE 1. Data

Latitude, °N	Longitude, °E	Datum	Error	Ridge Normal	Three-Plate Model	Importance	Reference	Description
					Eurasia-North America: Rates			
86.5	43.0	12	3	159	11.5	0.074	*Vogt et al.* [1979, fig. 3]	10 eastern-most profiles
84.9	7.5	13	3	132	12.9	0.065	*Feden et al.* [1979, fig. 2]	9 profiles
84.1	0.0	13.0	1.5	124	13.3	0.248	*Feden et al.* [1979, fig. 2]	12 profiles
83.4	-4.5	15	3	122	13.6	0.059	*Feden et al.* [1979, fig. 2]	11 profiles
73.7	8.5	17	4	119	15.7	0.023	*Vogt et al.* [1982, fig. 25]	rate-age plot
72.5	3.0	15	4	149	14.7	0.023	*Vogt et al.* [1982, fig. 25]	rate-age plot
71.8	-2.5	14	3	156	13.3	0.035	*Kovacs et al.* [1982]	5 profiles
69.6	-16.0	17.0	1.5	106	18.1	0.130	*Vogt et al.* [1980, fig. 2]	10 profiles
69.3	-16.0	17.5	2	104	18.1	0.073	*Vogt et al.* [1980, fig. 2]	8 profiles
68.5	-18.0	18.0	2	106	18.5	0.070	*Vogt et al.* [1980, fig. 2]	8 profiles
67.9	-18.5	18.0	1.5	103	18.6	0.122	*Vogt et al.* [1980, fig. 2]	15 profiles
61.6	-27.0	19.0	1.5	126	18.5	0.093	*Talwani et al.* [1971, fig. 5]	6 profiles
60.2	-29.1	19.0	1.5	126	18.6	0.092	*Talwani et al.* [1971, fig. 5]	5 profiles
44.5	-28.2	25	4	112	23.1	0.023	*NGDC; Atlantis II* 32-2	2 profiles
43.8	-28.5	24	3	108	23.5	0.043	NGDC; *Atlantis II* 32-2, *Conrad* 9-13	2 profiles
43.3	-29.0	23	3	108	23.5	0.044	NGDC; *Atlantis II* 32-2	2 profiles
42.9	-29.3	25.5	2	108	23.6	0.101	NGDC; *Atlantis II* 32-2	2 profiles
42.7	-29.3	23.0	2	90	23.8	0.109	NGDC; *Chain* 8-2	2 profiles
42.3	-29.3	23.5	2	85	23.4	0.110	NGDC; *Vema* 27-7, *Chain* 8-2	4 profiles
41.7	-29.2	24.5	3	90	23.9	0.051	NGDC; *Chain* 8-2, DSDP 94-GC	4 profiles
					Eurasia-North America: Transform Faults			
80.0	1.0	125.5	5	...	125.8	0.115	*Perry et al.* [1978]	PDR
78.8	5.0	127	10	...	127.9	0.029	*Perry et al.* [1978]	PDR
71.3	-9.0	114.0	3	...	113.5	0.231	*Perry et al.* [1978]	PDR
52.6	-33.2	95.9 (95.0)	3	...	96.3	0.133	*Searle* [1981, table 2] *Searle* [1981, plate 1]	Gloria
52.1	-30.9	95.5 (94.5)	2	...	97.4	0.292	*Searle* [1981, table 2] *Searle* [1981, fig. 5]	Gloria
					Eurasia-North America: Slip Vectors			
80.30	-1.93	125	20	...	123.7	0.007	*Dziewonski et al.* [1987*b*]	Oct. 8, 1986
80.20	-0.70	130	20	...	124.6	0.007	*Cook et al.* [1986]	Nov. 23, 1967
79.81	2.90	134	20	...	127.1	0.007	*Cook et al.* [1986]	Oct. 18, 1967
79.80	2.90	139	20	...	127.1	0.007	*Cook et al.* [1986]	Oct. 26, 1970
70.97	-6.86	116	20	...	114.7	0.005	*Cook et al.* [1986]	March 23, 1971
71.19	-8.03	113	15	...	114.1	0.009	*Dziewonski et al.* [1987*c*]	Nov. 20, 1979
71.23	-8.21	110	20	...	114.0	0.005	*Cook et al.* [1986]	Feb. 22, 1970
71.49	-10.36	106	20	...	112.7	0.005	*Cook et al.* [1986]	April 16, 1975
71.62	-11.51	111	15	...	112.0	0.009	*Dziewonski et al.* [1985*b*]	July 30, 1984
52.82	-34.25	98	10	...	95.8	0.012	*Bergman and Solomon* [1988]	Feb. 13, 1967
52.80	-34.20	101	20	...	95.8	0.003	*Engeln et al.* [1986]	July 5, 1965
52.70	-33.30	100	20	...	96.2	0.003	*Engeln et al.* [1986]	April 8, 1966
52.71	-32.00	98	10	...	96.9	0.012	*Bergman and Solomon* [1988]	Oct. 16, 1974
52.50	-31.85	103	20	...	97.0	0.003	*Engeln et al.* [1986]	Sept. 24, 1969
					Africa-North America: Rates			
36.8	-33.2	21.5	2	118	20.9	.073	*Macdonald* [1977, figs. 4,7]	5 profiles corrected for bathymetry and age-distance plot
36.8	-33.2	20.5	2	118	20.9	0.073	*Rabinowitz and Schouten* [1985]	1 profile
36.5	-33.7	22	3	122	20.5	0.030	*Rabinowitz and Schouten* [1985]	1 profile
36.0	-34.1	20	3	122	20.6	0.030	*Rabinowitz and Schouten* [1985]	1 profile
35.0	-36.5	21	4	97	22.1	0.021	*Le Douaran et al.* [1982, fig. 1]	1 profile
34.3	-37.0	21	3	119	21.5	0.030	*Le Douaran et al.* [1982, fig. 1]	1 profile
31.9	-40.5	23	4	118	22.2	0.018	*Rabinowitz and Schouten* [1985]	1 profile
30.9	-41.7	23	4	117	22.5	0.019	*Rabinowitz and Schouten* [1985]	1 profile
30.5	-41.9	22	3	112	23.0	0.035	*Rabinowitz and Schouten* [1985]	1 profile
29.6	-43.0	23	3	105	23.6	0.038	*Le Douaran et al.* [1982, fig. 1]	1 profile
27.5	-44.2	24	3	112	23.6	0.041	*Rabinowitz and Schouten* [1985]	1 profile
26.9	-44.5	26	4	106	24.1	0.024	*Rabinowitz and Schouten* [1985]	1 profile
26.2	-44.8	22	3	120	23.0	0.043	*McGregor et al.* [1977, fig. 3]	contour map
25.7	-45.0	24	4	115	23.7	0.025	*Rabinowitz and Schouten* [1985]	1 profile
25.3	-45.4	22.5	2	114	23.8	0.104	*Rabinowitz and Schouten* [1985]	1 profile

TABLE 1. (continued)

Latitude, °N	Longitude, °E	Datum	Error	Ridge Normal	Three-Plate Model	Importance	Reference	Description
25.1	-45.4	24.5	2	114	23.9	0.105	*Rona and Gray* [1980, figs. 4,7]	contour map and age-distance plot
24.5	-46.1	23	4	113	24.1	0.028	*Rabinowitz and Schouten* [1985]	1 profile
24.2	-46.3	24.5	2	105	24.6	0.112	*Rona and Gray* [1980, figs. 4,7]	contour map and age-distance plot
23.0	-45.0	25	4	98	24.8	0.029	*Rabinowitz and Schouten* [1985]	1 profile
22.8	-45.0	25.0	2	94	24.6	0.113	*Rabinowitz and Schouten* [1985]	1 profile
					Africa-North America: Transform Faults			
35.2	-35.6	104.5	2	...	102.8	0.221	*Roest et al.* [1984, table 1]	Gloria
33.7	-38.7	104.5	2	...	102.4	0.253	*Roest et al.* [1984, table 1]	Gloria
		(105.0)					*Bergman and Solomon* [1988, fig. 4]	
30.0	-42.4	101.5	3	...	101.7	0.128	*Roest et al.* [1984, table 1]	Gloria
23.7	-45.7	98.0	2	...	100.9	0.304	*Pockalny et al.* [1988, plate 1]	SeaBeam
		(98.5)					*Roest et al.* [1984, table 1]	Gloria
		(98.0)					*Bergman and Solomon* [1988, fig. 5]	
					Africa-North America: Slip Vectors			
35.14	-35.45	101	15	...	102.8	0.004	*Dziewonski et al.* [1988*a*]	July 14, 1980
35.41	-36.01	101	10	...	102.8	0.009	*Dziewonski et al.* [1983]	June 6, 1982
35.43	-36.03	102	20	...	102.8	0.002	*Dziewonski et al.* [1986]	April 29, 1985
35.35	-36.08	100	10	...	102.8	0.009	*Bergman and Solomon* [1988]	May 17, 1964
33.78	-38.46	102	15	...	102.4	0.004	*Dziewonski et al.* [1985*a*]	May 7, 1984
33.69	-38.60	103	15	...	102.4	0.004	*Dziewonski et al.* [1985*a*]	May 3, 1984
33.79	-38.64	101	10	...	102.4	0.010	*Bergman and Solomon* [1988]	March 28, 1976
28.74	-43.58	91	20	...	101.4	0.003	*Engeln et al.* [1986]	Jan. 21, 1969
23.83	-45.94	100	10	...	100.9	0.012	*Bergman and Solomon* [1988]	May 19, 1963
23.86	-45.57	100	10	...	100.9	0.012	*Bergman and Solomon* [1988]	March 26, 1980
23.81	-45.44	106	15	...	100.9	0.005	*Dziewonski et al.* [1988*b*]	Nov. 28, 1981
23.74	-45.17	102	15	...	100.9	0.005	*Dziewonski et al.* [1987*a*]	March 12, 1977
					Eurasia-Africa: Transform Faults			
36.9	-23.5	77.0	5	...	80.3	0.186	*Laughton et al.* [1972, p. 219]	Gloria
		(78.0)					*Laughton et al.* [1972, fig. 4]	
37.0	-22.6	85.0	3	...	83.1	0.401	*Laughton et al.* [1972, p. 218]	Gloria
		(86.0)					*Laughton et al.* [1972, fig. 4]	
37.1	-21.7	85.0	3	...	85.8	0.388	*Laughton et al.* [1972, p. 218]	Gloria
		(86.0)					*Laughton et al.* [1972, fig. 4]	
37.1	-20.5	90	7	...	89.4	0.098	*Searle* [1979, fig. 6] and *Laughton and Whitmarsh* [1974, fig. 4]	Gloria
					Eurasia-Africa: Slip Vectors			
37.75	-17.25	92	25	...	98.9	0.023	*Grimison and Chen* [1988]	Oct. 17, 1983
37.22	-14.93	130	25	...	105.8	0.043	*Grimison and Chen* [1986]	Dec. 30, 1970
36.96	-11.84	87	25	...	114.5	0.073	*Grimison and Chen* [1986]	Sept. 6, 1969
36.01	-10.57	129	25	...	119.1	0.103	*Grimison and Chen* [1988]	Feb. 28, 1969
35.99	-10.34	120	25	...	119.7	0.107	*Grimison and Chen* [1986]	May 5, 1969
36.23	-7.61	145	25	...	126.1	0.119	*Grimison and Chen* [1986]	Mar. 15, 1964

Rates are in mm/yr. Transform faults, slip vectors, and ridge normals are in degrees clockwise from north. Parenthesized values are estimates of transform azimuths that we made from published figures; they are not used in the inversion. Importances, calculated as described by *Minster et al.* [1974], measure the distribution of information among the data. NGDC, magnetic data obtained from the National Geophysical Data Center. PDR, precision depth recorder. DSDP, Deep Sea Drilling Project.

the Naval Research Laboratory (Figures 1 and 3) [*Vogt et al.*, 1979, 1980, 1982; *Feden et al.*, 1979. Twelve unusually good, high-amplitude profiles near the Yermak hotspot at the southwestern end of the Arctic Ridge (Figure 1) show the anomaly sequence clearly, and allow an excellent determination of spreading rate since 3 Ma. The new rates are 1–3 mm/yr faster than predicted by prior models (Figure 3). These small discrepancies are important for predicting the motion between Eurasia and North America along the continental part of the plate boundary. Magnetic data nearer the Laptev Sea along the Arctic Ridge have been published in contour map format [*Karasik*, 1974]. We omit these data here because we could not confidently identify anomaly 2′.

Both the best fitting and global Eurasian-North American vector found by *Minster and Jordan* [1978] give rates systematically slower than were observed south of Charlie-Gibbs transform. To investigate the cause of this discrepancy, we analyzed unpublished National Geophysical Data Center profiles from this region (Figure 5), and

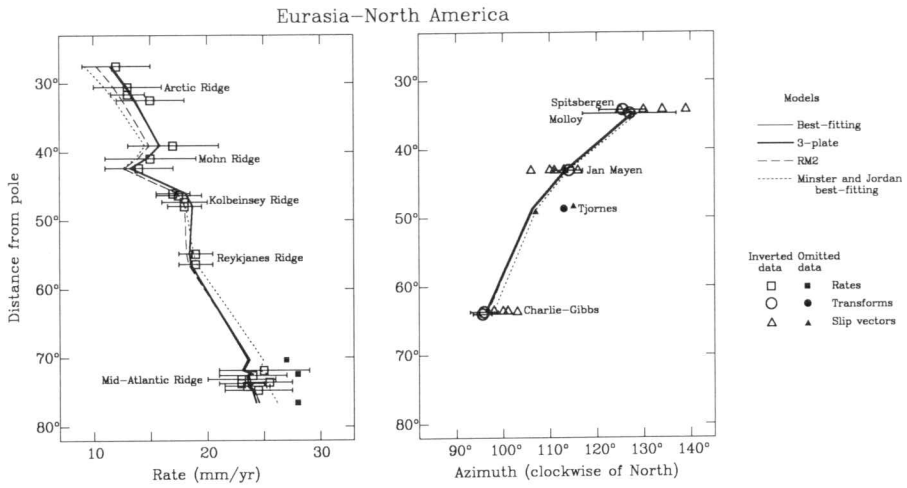

Fig. 3. Eurasia-North America plate motion data observed along the Arctic, Mohn, Kolbeinsey, Reykjanes, and Mid-Atlantic ridges are compared with rates and azimuths calculated from different plate motion models. The vertical axis shows the angular distance from our best fitting Eurasia-North America Euler pole. Squares show seafloor spreading rates determined from magnetic profiles, circles show observed transform fault azimuths, and triangles show observed slip vector azimuths. Symbols are open if used in our inversion, and solid if not. Rates (23–25.5 mm/yr) along the Mid-Atlantic Ridge (41–45°N) are 4 mm/yr slower than rates used by *Minster and Jordan* [1978] (solid squares). We did not invert *Cook et al.'s* [1986] slip vectors along the Tjornes transform fault (within the Iceland Platform) [*Saemundsson*, 1974; *Einarsson*, 1979] because its zone of seismicity is wide (80 km) and because it lacks a clear bathymetric expression. The thin solid line was calculated from our best fitting vector, the thick solid line from our self-consistent three-plate (Africa-Eurasia-North America) model, the long-dashed line from *Minster and Jordan's* [1978] RM2 global model, and the short-dashed line from *Minster and Jordan's* [1978] best fitting vector. Because the calculated rates are projected to ridge orthogonal, the calculated rate curves are jagged. The azimuth calculated from the three-plate model is 7° counterclockwise of Saemundsson's estimate of the strike of the Tjornes fault, which suggests that some extension occurs within the broad zone of seismicity near the fault. The slip vectors tend to be a few degrees counterclockwise of the azimuths of the left-lateral slipping Jan Mayen transform fault, and a few degrees clockwise of the azimuths of the right-lateral slipping Spitsbergen and Charlie-Gibbs transform faults.

found rates 2–5 mm/yr slower than those used by *Minster and Jordan* [1978] and *Chase* [1978]. The prior misfit thus was caused by a bias in the old data. The new well-distributed rates give an Euler vector confidence ellipse with a major axis 3 times smaller than those of prior studies (Figure 4). Our best fitting vector lies about midway between *Chase's* [1978] and *Minster and Jordan's* [1978] global and best fitting vectors (Figure 4).

We searched the Eurasian-North America plate motion data for evidence of another plate boundary, but found no significant systematic misfits. In particular the improvement in fit was insignificant when we divided the conventionally defined Eurasian plate into two plates: a Eurasian plate and a Spitsbergen microplate. Thus if a Spitsbergen microplate exists, its motion relative to Eurasia is less than about 3 mm/yr, which numerical experiments suggest is the slowest motion resolvable by our test.

Slip vectors along each of the three major well-mapped transform faults show a small systematic bias relative to the presumably accurately mapped transform fault azimuths. The slip vectors tend to be rotated a few degrees clockwise relative to the right-lateral slipping Charlie-Gibbs and Spitsbergen transforms, and a few degrees counterclockwise relative to the left-lateral slipping Jan Mayen transform. Because the bias changes sign between right-lateral and left-lateral faults, it cannot be explained by a recent change in direction of plate motion. It also cannot be explained by the fanning of transform fault trends relative to the directions predicted by plate motion models, as recently documented for Africa-North America transform faults by *Roest et al.* [1984], because the slip vectors are rotated in the same sense with respect to both the plate motion models and the observed transform fault azimuths (Figure 3). The data are probably too sparse to make firm generalizations, but the data that appear to be the most biased tend to be from smaller earthquakes and from older focal mechanisms, some of which are based only on P wave first motions. The former observation suggests a possible tectonic origin of the bias: that the small earthquakes occur on faults short enough that they need not be parallel to plate motion, whereas the latter observation suggests the focal mechanisms are biased relative to the true direction of slip, which could possibly be explained by lateral velocity heterogeneities associated with the presence of slower velocities in the hot crust and mantle beneath spreading ridges. Any convincing explanation of this small bias will need more data and analysis than presented here.

Africa-North America Motion

Long- versus short-offset transform faults. Several studies have shown that the short-offset transform faults are in many places oblique to the direction of plate motion. The trend (N55°E) of the active segment of the short-offset (20 km) Kurchatov transform is oblique to the fracture zone [*Searle and Laughton*, 1977], which roughly

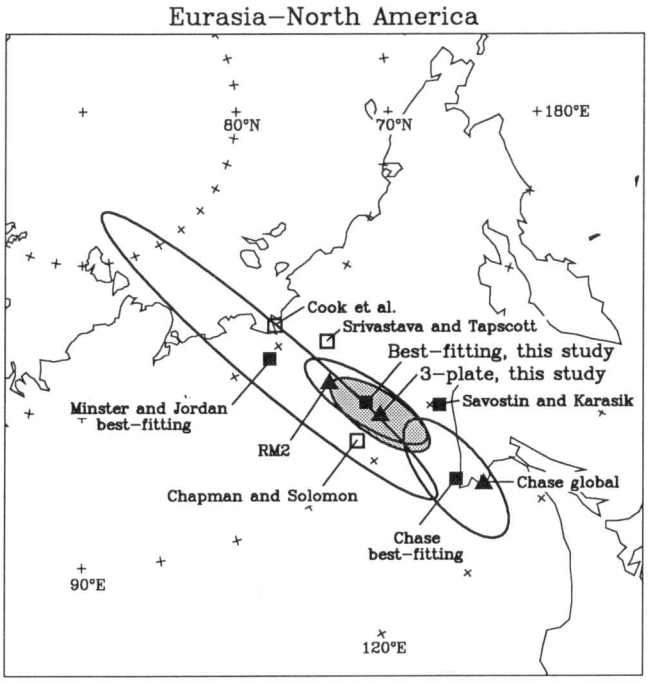

Fig. 4. Poles and 1-σ confidence limits for Eurasia-North America motion. Prior poles include those of *Chapman and Solomon* [1976], *Chase* [1978], *Minster and Jordan* [1978], *Savostin and Karasik* [1981], *Cook et al.* [1986], *Srivastava and Tapscott* [1986], and this study. The 1-σ confidence limits are shown for the *Minster and Jordan* [1978] best fitting vector, *Chase* [1978] best fitting vector, our best fitting vector, and our three-plate model vector (shaded). Equal-area projection.

parallels the plate motion direction (S83°E). The fracture zone consists of short, en echelon, northeast trending scarps, which form a zigzag pattern. This transform-fracture zone geometry suggests that the northeast trend of the active transform is not parallel to the direction of plate motion [*Searle*, 1986].

In the eastern 20 km of the Vema transform, the transform fault zone (the main zone of displacement) is broad with many splays, and cuts across the inside corner of the transform [*Macdonald et al.*, 1986]. Within the 10 km nearest the ridge-transform intersection the transform fault zone and transform valley trend 5–10° clockwise of their trend in the central part of the transform, suggesting that transforms with 20 km or less offset are likely to be 10–20° leaky.

Collette et al. [1979] find that short-offset transforms on the Mid-Atlantic Ridge between 10°N and 40°N are not parallel to plate motions, and always have a leaky azimuth. The azimuth of the short-offset (15 km) Thirteen-Fortyfive transform, which offsets the ridge left laterally, is ~25° clockwise of the long-offset Vema transform and the predicted plate motion. The azimuths of transforms A and B (FAMOUS area), which offset the ridge right laterally, are ~15° counterclockwise of the Oceanographer and the predicted plate motion. In contrast, we find that the accurately determined azimuths of long-offset transforms between 10°N and 40°N are within a few degrees of the plate motion directions determined from internally consistent plate motion models.

Gloria side scan studies of several long-offset North Atlantic transforms reveal a straight, narrow fault or zone of faults continuous along the transform, which are interpreted as taking up all the displacement between the plates [*Roest et al.*, 1984; *Searle*, 1986; *Parson and Searle*, 1986]. Within the Oceanographer the transform fault zone shows no sign of reorientation to the direction of the transforms A and B. Seismic sections across the Vema show that faulting within the top 200–500 m of sediment is confined to a 500-m-wide zone, showing that the transform fault zone is stable over 200,000–500,000 years [*Eittreim and Ewing*, 1975; *Bowen and White*, 1986]. This observation suggests that other principal transform displacement zones reflect motion over the past several hundred thousand years and have not been reoriented.

It thus appears that very short-offset transforms, such as the Kurchatov, are ~45° oblique to the direction of plate motion. Slightly longer transforms, such as transforms A and B, are ~15° oblique to plate motion, whereas long-offset transforms are parallel to plate motion [*Macdonald*, 1986]. The critical value of offset between oblique and parallel transforms appears to be between 25 and 35 km [*Searle*, 1986]. To be conservative, we exclude from our data set transform faults with offsets less than 35 km, although transforms with slightly

TABLE 2. Euler Vectors

Model	Vector			Error Ellipse			
	Latitude °N	Longitude °E	ω deg./m.y.	Azimuth, deg.	Semi-Major Axis, deg.	Semi-Minor Axis, deg.	σ_ω, deg./m.y.
			Eurasia-North America				
Best fitting	63.2	134.5	0.228	168	4.8	1.4	0.011
Three-plate	62.1	134.6	0.224	169	4.1	1.4	0.008
			Africa-North America				
Best fitting	73.7	94.8	0.222	140	14.7	1.4	0.014
Three-plate	79.1	64.6	0.236	102	5.2	1.0	0.010
			Africa-Eurasia				
Best fitting	21.4	-20.5	...	176	8.0	0.7	...
Three-plate	18.8	-20.3	0.104	176	7.6	0.8	0.018
Africa-North America plus North America-Eurasia	8.0	-9.5	0.068	139	32.7	12.8	0.036

The first plate moves counterclockwise relative to the second. Standard error ellipses are specified by the azimuth of the semi-major axis and length of the semi-major and semi-minor axes.

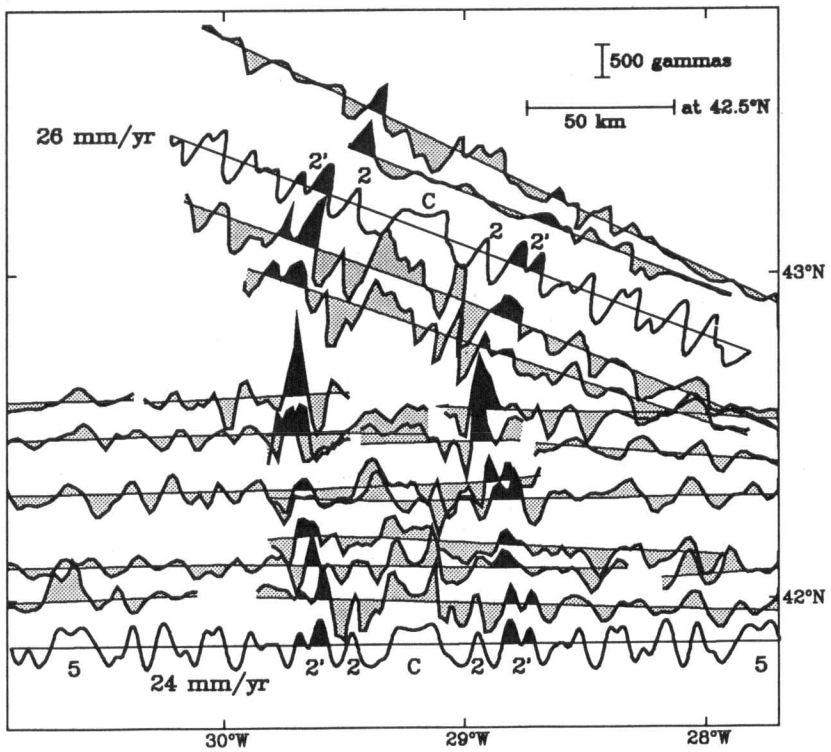

Fig. 5. Previously unpublished magnetic profiles (cruises *Chain* 82, *Vema* 2707, *Atlantis II* 32-1, from the National Geophysical Data Center) crossing the Mid-Atlantic Ridge north of the Azores Triple Junction. Synthetic profiles (unshaded) for 24 and 26 mm/yr fit the observed profiles (shaded) well. Anomaly 2′ is shaded black. The two synthetic profiles (unshaded) assume a 2-km seafloor depth, 500-m-thick magnetic layer, 0.01-emu/cm^3 magnetization, and a 1-km transition width.

shorter offsets may eventually prove also to be reliable indicators of plate motion direction.

Data and results. New, accurate, Gloria-surveyed azimuths of the Oceanographer, Hayes, Atlantis, and Kane transforms accurately measure the direction of Africa-North America motion (Table 1, Figure 6). The four new transform azimuths require the pole to lie within a narrow region elongated orthogonal to the transforms (Figure 7). Many new magnetic profiles improve the accuracy of the rates. The rates observed along the entire boundary are systematically ~2 mm/yr slower than predicted by RM2 (Figure 6). We determined 13 rates from many surface magnetic and aeromagnetic profiles compiled by *Rabinowitz and Schouten* [1985]. Deep-tow magnetics in the FAMOUS region constrain rates along the northern part of the plate boundary [*Macdonald*, 1977], whereas the data of *Rona and Gray* [1980] constrain rates along the southern part of the plate boundary. The 25 mm/yr rates we determined from the profiles of *Rabinowitz and Schouten* [1985] south of the Kane Fracture Zone are slower than the 28 mm/yr rate for the same region found by *Purdy et al.* [1979] in their study of a few Deep Sea Drilling Project (DSDP) profiles. Because *Purdy et al.* [1979] determined rates over a longer age interval than used here, the difference may be caused by a recent slowing of spreading.

The new data for this boundary give a best fitting vector with confidence limits that are several times smaller than found in prior studies (Figure 7). The best fitting vectors from prior studies lie outside the confidence limits of the new vector. However, prior global vectors differ insignificantly from our new best fitting vector, which suggests that biases in the old azimuth data may have caused the nonclosure about the Azores Triple Junction, as discussed further below.

As was true for the Eurasian-North American transform faults, slip vectors along the major well-mapped transform faults are biased relative to the presumably accurately mapped transform fault azimuths. The slip vectors are rotated clockwise relative to the right-lateral slipping Kane transform, and counterclockwise relative to the left-lateral slipping Oceanographer and Hayes transforms.

Africa-Eurasia Motion

We use four azimuths along the Gloria fault and six slip vectors along the eastern Azores-Gibraltar Ridge to describe Africa-Eurasia motion (Figures 2 and 8). If treated as a transform fault, the Gloria fault strongly constrains the longitude of the Africa-Eurasia pole (Figure 9). Earthquake mechanisms along the eastern Azores-Gibraltar Ridge show strike-slip faulting near the Gloria fault and thrust faulting near Gibraltar. The azimuths of Africa-Eurasia slip vectors agree with the Gloria fault azimuths. No rates have been determined from magnetic lineations paralleling the Terceira rift, which is the only place along the boundary where the seafloor is thought to spread [*Searle*, 1980, Figure 5].

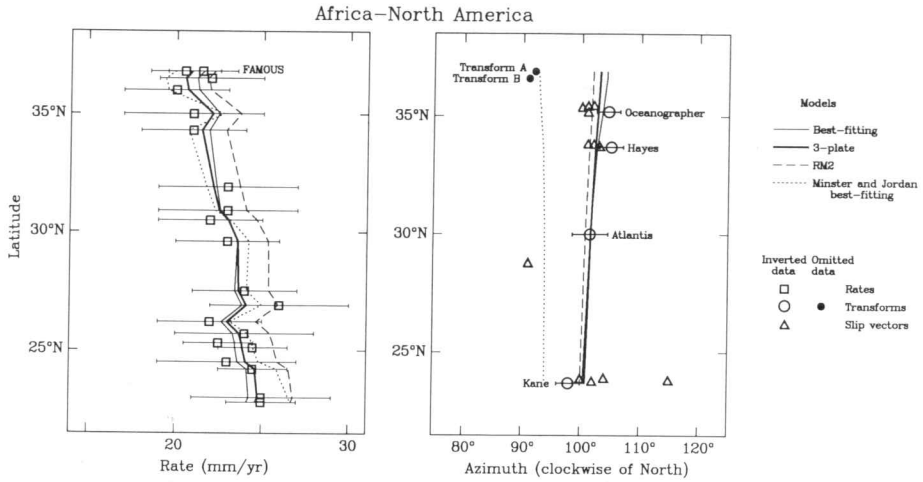

Fig. 6. Africa-North America plate motion data observed along the Mid-Atlantic Ridge are compared with rates and azimuths calculated from different plate motion models. Squares show seafloor spreading rates determined from magnetic profiles, circles show observed transform fault azimuths, and triangles show observed slip vector azimuths. Symbols are open if used in our inversion, and solid if not. The azimuths of transforms A and B were used by *Minster and Jordan* [1978], but omitted by us because the transform faults have short ridge offset. The thin solid line was calculated from our best fitting vector, the thick solid line from our self-consistent three-plate (Africa-Eurasia-North America) model, the long-dashed line from *Minster and Jordan's* [1978] RM2 global model, and the short-dashed line from *Minster and Jordan's* [1978] best fitting vector. Because the calculated rates are projected to ridge orthogonal, the calculated rate curves are jagged. The slip vectors tend to be a few degrees counterclockwise of the azimuths of the left-lateral slipping Oceanographer and Hayes transform faults, and a few degrees clockwise of the azimuths of the right-lateral slipping Kane transform fault.

The revised Africa-Eurasia slip vectors include six mechanisms from *Grimison and Chen* [1986, 1988]. Their mechanisms, determined using body waveform inversion [*Nabelek*, 1984], should be better constrained than older solutions. We only use mechanisms on the eastern Azores-Gibraltar Ridge within the 50-km-wide zone we take to be the Africa-Eurasia boundary, and exclude mechanisms off the boundary, such as the May 15, 1975, earthquake [*Lynnes and Ruff*, 1985]. We could unambiguously determine which nodal plane was the fault plane for all but two mechanisms. Both of these mechanisms were thrust faults and for both we assumed that the shallower dipping plane was the fault plane. We used the centroidal solutions for two mechanisms that *Grimison and Chen* [1986, 1988] model with two subevents. We excluded mechanisms of pre-1964 earthquakes unrecorded by the World-Wide Standard Seismograph Network (WWSSN), such as the November 25, 1941, earthquake used in prior plate motion studies. We also excluded several mechanisms on the Terceira rift. Two were normal faulting events, and the aftershocks of a third event, the January 1, 1980, strike-slip earthquake, suggest that the fault plane is nearly normal to the expected direction of motion [*Hirn et al.*, 1980]. The choice of some mechanisms, fault planes, and associated slip vectors from individual events is arbitrary; however, the best fitting pole depends only weakly on these choices. East of ~22°W, the best fitting pole determined from the revised data suggests a direction of Africa-Eurasia motion counterclockwise of the predictions of RM2.

An important decision in determining the data set is how great a length to assume for the Gloria fault. The longer the fault, the better its curvature is determined, and the stronger the constraint on the latitude of the Euler pole. *Searle* [1979] found a pole from a small circle that best fits the Gloria fault between 24°W and 21°W, but his line drawings suggest that the lineations continue eastward to 18.5°W. However, *Laughton and Whitmarsh* [1974] argue that the fault extends eastward along 37.2°N only to 20°W, where the Africa-Eurasia boundary bends northward to a point near 38°N at 18°W. We used Gloria fault azimuths at three unambiguous locations of the fault (23.5°W, 22.6°W, and 21.7°W), and one location near its east end (20.5°W). The latitude of our best fitting pole, although constrained more strongly by the eastern Azores-Gibraltar slip vectors than by the variation in the strike of the Gloria fault, is similar to Searle's pole from only the Gloria fault.

Grimison and Chen [1986] note a consistent north-northwest orientation of the P axis of focal mechanisms along the eastern Azores-Gibraltar Ridge, and suggest that southwesterly extension occurs at the Terceira rift and north-northwest compression occurs near Gibraltar. If these P axes describe the direction of Africa-Eurasia motion, then the pole must lie near the boundary at ~35°N, which is inconsistent with the observed small curvature of the Gloria fault. Our pole, south of the pole location implied by *Grimison and Chen's* [1986] model, fits both the small curvature of the Gloria fault and the slip vectors along the eastern Azores-Gibraltar Ridge; it does not predict motion parallel to the P axes of strike-slip mechanisms (Figures 2 and 8; also see Figure 11).

THREE-PLATE MODEL AND CLOSURE

The closure-enforced, three-plate model fits the data well, without systematic misfits. The rates and azimuths

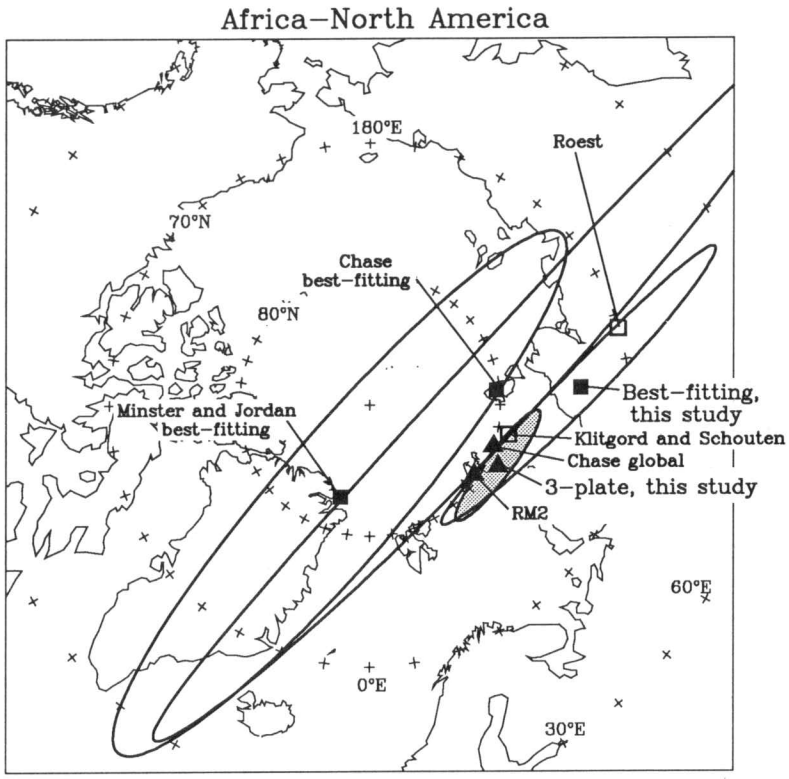

Fig. 7. Poles and 1-σ confidence limits for Africa-North America motion from *Chase* [1978], *Minster and Jordan* [1978], *Klitgord and Schouten* [1986], *Roest* [1987], and this study. The 1-σ confidence regions are shown for the *Minster and Jordan* [1978] best fitting vector, *Chase* [1978] best fitting vector, our best fitting vector, and our 3-plate model vector (shaded). Equal area projection.

calculated from the best fitting and three-plate models are similar to one another (Figures 3, 6, and 8); the three-plate vectors differ insignificantly from the best fitting vectors. The constraints from closure narrow the confidence limits of the Africa-North America pole (Figure 7). The data along the Africa-Eurasia boundary do not give the rate of motion along the boundary. Nevertheless, from differences in Mid-Atlantic Ridge spreading rate north and south of Azores, the rate along the Azores-Gibraltar Ridge is predicted to be ~4 mm/yr: slow but ~50% faster than predicted by RM2. The three-plate model gives a more southerly Africa-Eurasia pole, and thus less variation in direction of motion along the boundary than prior models. In particular, the direction of convergence near Gibraltar is predicted to be ~15° counterclockwise of the direction predicted by RM2.

The data accurately describe the motion along each plate boundary and provide a strong test of plate circuit closure. As a preliminary test of the consistency of the data, we determined an Africa-Eurasia Euler vector by

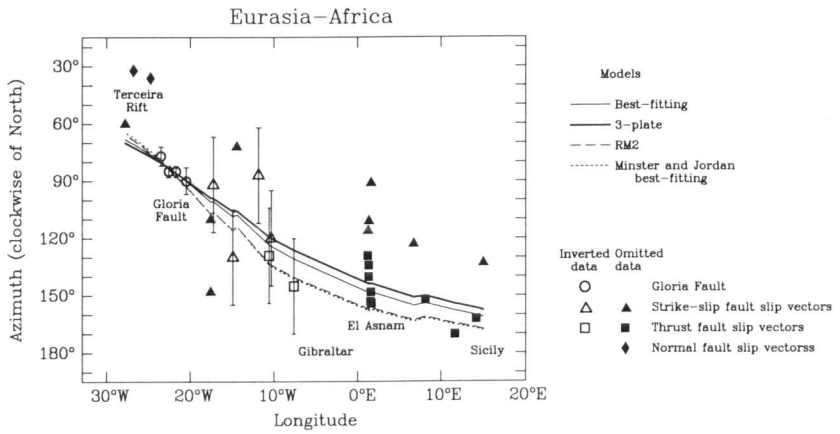

Fig. 8. Plate motion data and models for Africa-Eurasia. Circles show fault azimuths along the Gloria fault. Triangles are slip vectors from strike-slip faulting earthquakes, squares are slip vectors from thrust faulting earthquakes, and diamonds are slip vectors from normal faulting earthquakes. Slip vectors are open if we included them in our inverted data set, and solid if we omitted them.

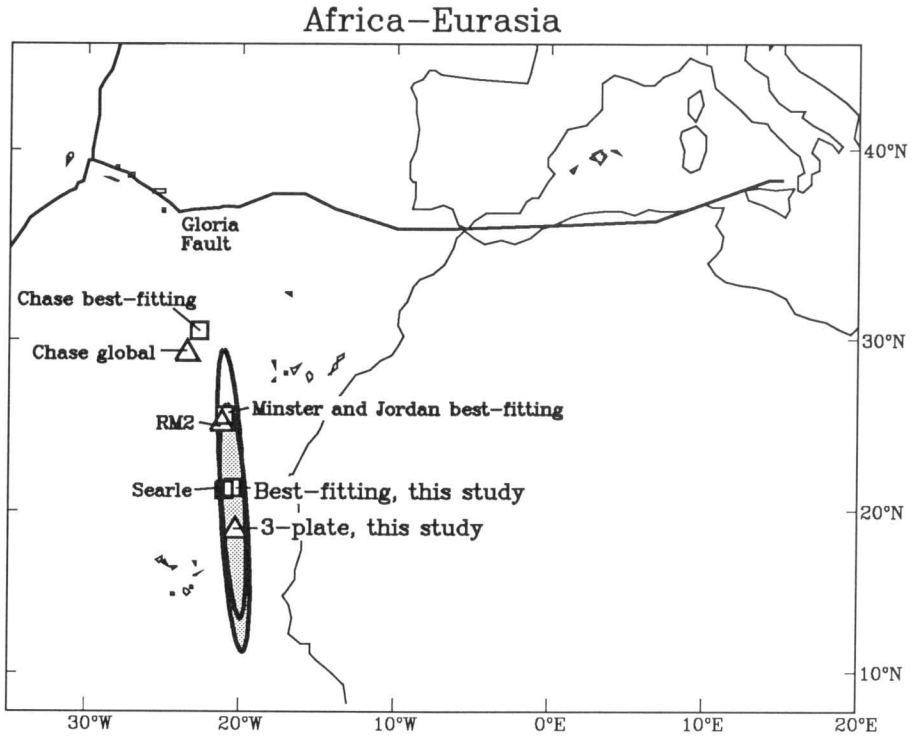

Fig. 9. Poles and 1-σ confidence limits for Africa-Eurasia motion from *Chase* [1978], *Minster and Jordan* [1978], *Searle* [1979, 1980], and this study. Equal-area projection.

summing the Eurasia-North America and North America-Africa Euler vectors. The confidence limits of the Africa-Eurasia Euler vector estimated from closure, like all other confidence limits in this paper, were determined by linear propagation of errors (appendix). The "predicted" Africa-Eurasia vector thus determined from our data differs from those we determined by the same method from the data of *Minster and Jordan* [1978] and *Chase* [1978] (Figure 10). The 1-σ ellipsoidal error region of our predicted vector overlaps the 1-σ ellipsoidal error region of our best fitting vector, which suggests our data are consistent with closure. In contrast, the predicted vector we determined from Minster and Jordan's data excludes the error region of the best fitting vector, suggesting nonclosure. The small reduced chi-square (0.19) suggests that the model agrees reasonably with the data, and that we have probably systematically overestimated the errors in the data. We obtained a value of F=3.2 from the F ratio test for plate circuit closure, which is less than the value (4.9) that would show nonclosure significant at the 1% risk level. Thus the data are consistent with closure.

DISCUSSION

Comparison With Slip Vectors Between Gibraltar and Sicily

In our inversion we have omitted slip vectors from the line of seismicity that runs east of Gibraltar, across North Africa to Sicily. As *McKenzie* [1972] has stressed, it is important to test whether the plate motion model determined from Atlantic and Arctic data is consistent with the slip vectors between Gibraltar and Sicily, which are the only slip vectors in the Mediterranean region that may reflect motion between Eurasia and Africa (Figures 2, 8, and 11). East of Sicily, earthquakes typically reflect motion of microplates or zones of distributed deformation [*McKenzie*, 1972]. Figure 8 shows the direction of slip predicted by our three-plate model and the orientation of the slip vectors determined from the 14 Harvard centroid moment tensor (CMT) solutions available for this region. For thrust mechanisms, we took the fault plane to be the shallower dipping nodal plane, except for events at El Asnam (36.2°N, 1.4°E, in the Atlas Mountains of northern Algeria (Figure 2)), where we always took the northwest dipping plane. Five vectors from strike-slip mechanisms are in only fair agreement with the predictions, but the other nine mechanisms are thrust faults with slip vectors in reasonable agreement with the predicted direction of motion (Figure 8). P wave modeling of the October 10, 1980, El Asnam earthquake [*Yielding*, 1985] suggests the African plate moves northwest relative to the Eurasian plate along a fault plane dipping moderately to the north. The geodetic survey of *Ruegg et al.* [1982] also suggests the El Asnam earthquake resulted from northwest-southeast motion. We thus conclude that our model is consistent with the slip vectors and other observations, and that any independent motion of continental blocks relative to the major plates (e.g., the motion of the Alboran plate relative to Eurasia [*Udias et al.*, 1976]) is negligible. Our model and the CMT slip vectors both suggest Africa-Eurasia motion systematically counterclockwise of prior models. The slip rate (4–7 mm/yr) is much less than early models of Africa-Eurasia motion [e.g., *McKenzie*, 1972], but comparable to later models [e.g., *Chase*, 1978; *Minster and Jordan*, 1978].

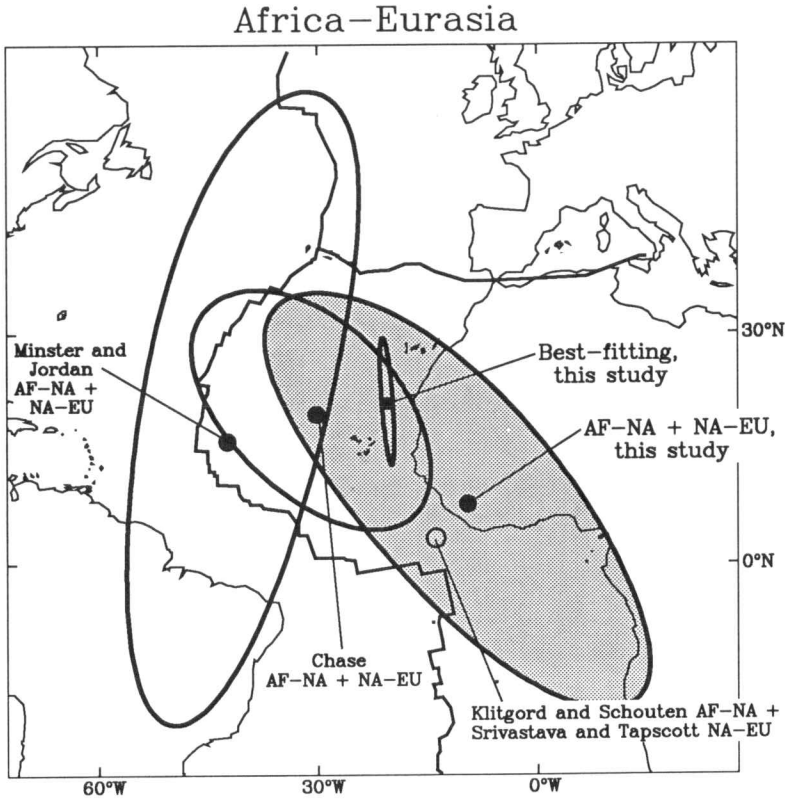

Fig. 10. Africa-Eurasia Euler vectors calculated by adding Africa-North America and North America-Eurasia vectors are compared with the best fitting pole. Poles are shown that were calculated by summing Africa-North America and North America-Eurasia rotations from (1) *Chase* [1978], (2) *Minster and Jordan* [1978], (3) the Africa-North America rotation of *Klitgord and Schouten* [1986] with the North America-Eurasia rotation of *Srivastava and Tapscott* [1986], and (4) this study. The 1-σ confidence regions are shown for the *Minster and Jordan* [1978] predicted vector, *Chase* [1978] predicted vector, our predicted vector (shaded), and our best fitting vector. Our best fitting and closure-predicted poles overlap, consistent with closure of the plate circuit. Minster and Jordan's closure-predicted pole excludes both the new and their old (not shown) best fitting poles. Equal-area projection.

Comparison of Slip Vector With Transform Fault Azimuths

Generally the data are well fit except for a small systematic misfit to the slip vectors, as noted above. Figure 12 summarizes the comparison of the azimuths of slip vectors to the azimuth of the corresponding well-mapped transform fault. Slip vectors are on average 5° clockwise of transform fault azimuths on right-lateral slipping transforms and 4° counterclockwise of transform fault azimuths on left-lateral slipping transforms. Combining these two data sets gives a mean slip vector bias of 5°. The accuracy of individual slip vectors is poorly known. If the errors in slip vector azimuths are uncorrelated and the 95% error limits have a nominal value of ±5°, the formal 95% confidence limits on the mean slip vector bias are ±1°. Similarly, if we assume a nominal 95% error limit value of ±10°, the formal 95% confidence limits on the mean slip vector bias are ±2°. If we instead calculate the confidence limits from the scatter in the observed slip vector residuals, the formal 95% confidence limits on the mean slip vector bias are ±2°. A discrepancy this small could have many possible explanations, including a bias in focal mechanisms due to the lateral velocity heterogeneity associated with low-velocity mantle beneath spreading centers or a tendency for small earthquakes to rupture along faults not parallel to the transform fault, perhaps because of the near-transform fault stress field. Alternatively, the bias may be caused by some small unknown source of systematic error or because the errors between different focal mechanisms are correlated. In any event the data suggest that small systematic misfits of plate motion models to transform fault slip vectors elsewhere in the world should be interpreted with caution [cf. *DeMets et al.*, 1988].

Plate Circuit Closure

We find, in contrast to prior studies, that the plate motion data are consistent with closure about the Azores Triple Junction. The nonclosure found by *Minster and Jordan* [1978] results from the use of azimuths of short-offset transform faults, which give unreliable directions of plate motion. Long-offset transforms, however, appear to record the direction of plate motion accurately. The azimuth of six of the seven long-offset transform faults surveyed by Gloria or Sea Beam are fit by our three-plate model within 2°, and the seventh (the Kane transform) is fit within 3°. That the seafloor south and west of the Kane transform fault may be part of a diffuse plate boundary dividing the North American and South American plates [*Minster et al.*, 1974; *Minster and Jordan*, 1978;

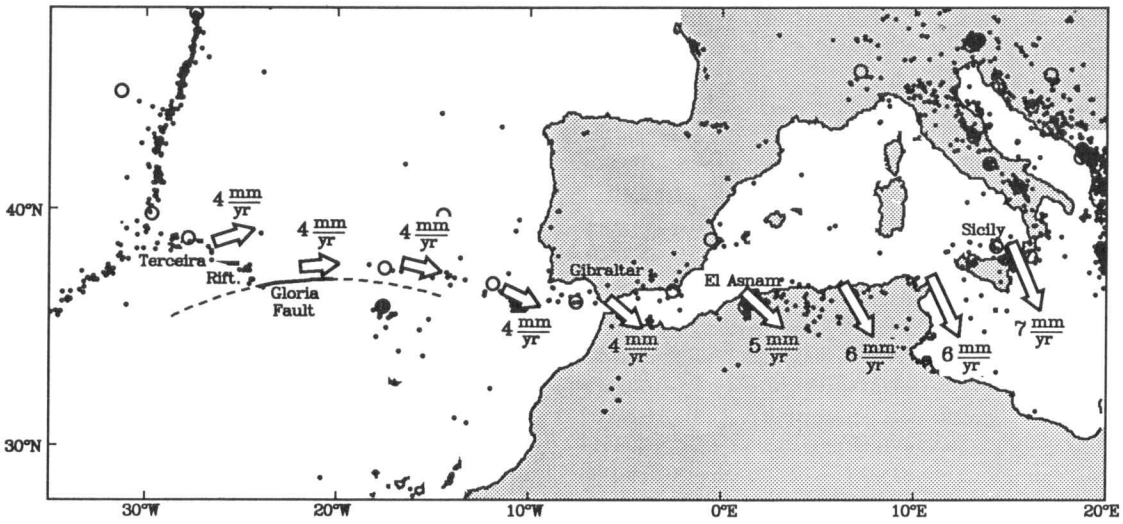

Fig. 11. Relative motion of Africa and Eurasia. Arrows show the motion of a location on the Africa plate (at tails of arrows) relative to the Eurasia plate. A small circle arc (dashed), centered at the three-plate Eurasia-Africa pole, well fits the Gloria fault.

Chase, 1978; *Stein and Gordon*, 1984] may cause the small but significant misfit to the azimuth of the Kane (D. F. Argus and R. G. Gordon, manuscript in preparation 1988). Aside from the misfit of the Kane azimuth, closure shows the data are consistent with the rigid plate hypothesis and with the Gloria fault being a true transform fault, suggesting that transform faults in unusual (i.e., not offsetting two spreading ridges) tectonic settings give reliable directions of plate motion. The only possible reservation about the transform fault interpretation of the Gloria fault is now its lack of seismicity (Figure 2). However, the lack of seismicity does not

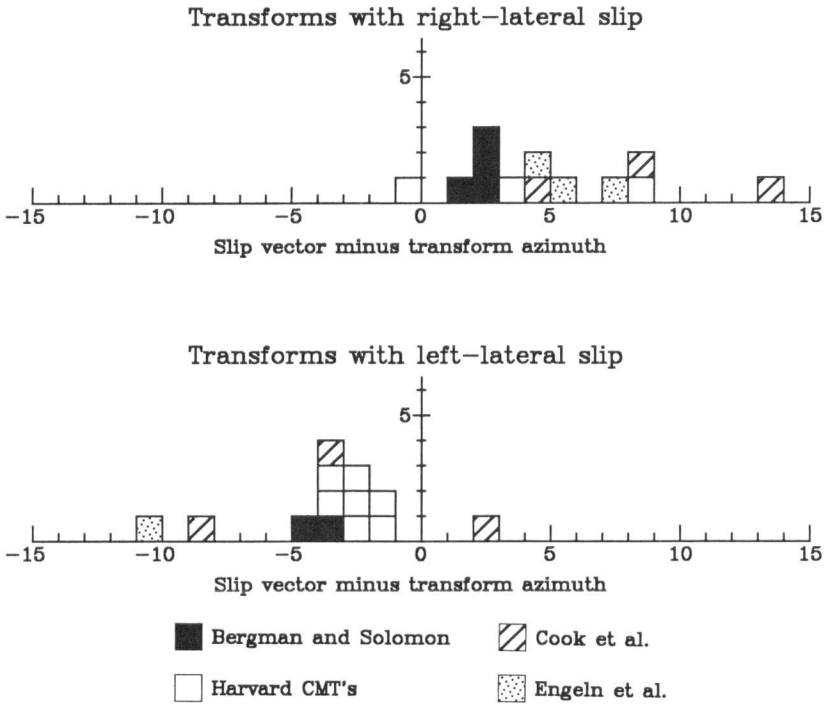

Fig. 12. Comparison of the azimuths of slip vectors to the azimuth of the corresponding well-mapped transform fault. At top, the azimuth of the slip vector minus the azimuth of the corresponding well-mapped transform fault is shown for right-lateral slipping transforms. At bottom, the azimuth of the slip vector minus the azimuth of the corresponding well-mapped transform fault is shown for left-lateral slipping transforms. Slip vectors are on average 5° clockwise of transform fault azimuths on right-lateral slipping transforms and 4° counterclockwise of transform fault azimuths on left-lateral slipping transforms. For 1 slip vector on a short-offset transform of unknown trend, we compare the slip vector with the three-plate model. Slip vectors are from *Bergman and Solomon* [1988], the Harvard CMT solutions, *Cook et al.* [1986], and *Engeln et al.* [1986].

necessarily imply fault inactivity, as illustrated by the seismic quiescence of the segments of the San Andreas Fault that ruptured in the great 1857 and 1906 earthquakes [*Allen*, 1981]. Motion along the Gloria fault may be aseismic or the recurrence interval between large earthquakes may be longer than the 75-year instrumental record, as suggested by the fault's meager slip rate of 4 mm/yr (in contrast to the San Andreas fault, which has a slip rate nearly 10 times faster).

CONCLUSIONS

The excellent, well-distributed plate motion data now available permit current Africa-Eurasia-North America motions to be determined accurately. Short-offset transform faults give unreliable and biased directions of plate motion, but the several long-offset transform faults that have been surveyed by Gloria or Sea Beam or both give directions that are consistent within a few degrees. The new high-quality transform fault azimuth data permit us to recognize a small bias in slip vectors from earthquakes occurring on Arctic, and North and Central Atlantic transform faults. Slip vectors tend to be a few degrees clockwise of plate motion on right-lateral slipping transform faults and a few degrees counterclockwise of plate motion on left-lateral slipping transforms. If there is an independent Spitsbergen microplate, its motion relative to Eurasia is less than ~3 mm/yr. The data are consistent with the Gloria fault being a true transform fault, despite its unusual tectonic setting. The data are also consistent with plate circuit closure and thus plate rigidity to within a few mm/yr (when averaged over a few million years). Moreover, the plate motion model accurately predicts the direction of slip on thrust earthquakes between Gibraltar and Sicily, suggesting that any motion of Eurasian microplates is much smaller than the 4–7 mm/yr rate of motion between Africa and Eurasia.

APPENDIX: METHODS

We analyze plate motion data on three tiers. At the lowest tier we analyze bathymetric data and maps, and magnetic profiles to obtain spreading rates and transform fault trends, and their associated confidence limits. We evaluate slip vectors from focal mechanisms determined by others and estimate their confidence limits. At the middle tier we analyze all plate motion data along a single plate boundary, find best fitting Euler vectors, examine the internal consistency of data, and compare the results to those found in prior studies. At the highest tier we test whether data from three separate plate boundaries are mutually consistent, i.e., consistent with plate circuit closure. Below we describe the methods of analysis adopted for each tier.

Lowest Tier: Spreading Rates, Transform Trends, and Slip Vectors

We used three types of plate motion data: spreading rates from marine magnetic profiles, trends of transform faults, and slip vectors from earthquake focal mechanisms. The data include 40 spreading rates derived from ~150 marine magnetic anomalies profiles, 13 transform fault azimuths, and 25 earthquake slip vectors (Table 1, Figure 1).

Spreading rates. For each magnetic profile we used standard techniques [*Schouten and McCamy*, 1972] to generate a series of synthetic magnetic profiles at 0.5 or 1 mm/yr increments of full spreading rate using the *Harland et al.* [1982] time scale. We adopted the rate that best fit each observed profile at the center of the anomaly 2′ sequence (2.92–3.15 Ma). This 3-m.y. averaging interval is shorter than in prior studies of current Arctic and North Atlantic plate motions [e.g., *Minster and Jordan*, 1978], which typically averaged rates over longer intervals because of the difficulty in identifying anomaly 2′ in older data. The best profiles crossing the Mid-Atlantic, Kolbeinsey, and Reykjanes ridges show the characteristic 2′ double peak on both sides of the ridge (Figure 5). On many profiles, however, especially those across the slow spreading Arctic Ridge, anomaly 2′ appears as a single broad positive anomaly. Rates are determined either from an individual profile, or from averaging the rates from several, closely spaced profiles.

The errors assigned to spreading rates depended on the number of profiles averaged to obtain a rate, the reproducibility of rates when different co-authors examined the same profile, and the subjectively estimated precision with which we could determine the rate from an individual profile. The error assigned to an individual profile ranged from 2 mm/yr for profiles with a complete, easily identified sequence of anomalies through 2′, to 4 mm/yr for profiles with an incomplete sequence, tenuous anomaly identifications, or with suspected ridge jumps. Although we could identify the entire sequence including the central anomaly, anomaly 2, and 2′ on only three of the 16 profiles used alone to give a rate, we could unambiguously identify the central anomaly and anomaly 2′ on 10 of the 16 profiles, and make reasonable fits, consistent with nearby profiles, to the remaining six profiles. The narrow 2–4 mm/yr range of assigned errors suggests that the Euler vectors we determine are not strongly affected by our weighting of these data.

Smaller errors of 1.5–2 mm/yr were assigned to 10 rates from averages of several closely spaced profiles. Closely spaced profiles allow fracture zones and propagating rifts to be identified, eliminating two sources of error on isolated profiles. Averaging rates from closely spaced profiles reduces the error of the mean rate for a group of profiles, giving a single datum that we weighted more (i.e., assigned a smaller error) than a rate from an isolated profile. Although the formal confidence limits of these averages were 1 mm/yr or less, we arbitrarily adopted a floor of 1.5 mm/yr for the smallest error we assigned. Our intent is to allow for possible systematic errors, which include wrong correlation of anomalies because of unrecognized fracture zones or propagating rifts, sloping reversal boundaries, or limitations of the simple, single-layered, two-dimensional block model we used to compute synthetic anomalies.

All but six rates were determined from a comparison of a profile or profiles to synthetic profiles we generated (Table 1). Two of these six exceptions are from a contour map and age-distance plot [*Rona and Gray*, 1980], one is from profiles inverted for magnetization and an age-distance plot [*Macdonald*, 1977], one is inferred from

a contour map [*McGregor et al.*, 1977], and two are based on rate-age plots [*Vogt et al.*, 1980]. Errors of 2 mm/yr were assigned to the *Rona and Gray* [1980] and *Macdonald* [1977] rates because two methods gave the same rate within 1 mm/yr, and the data seemed comparable to rates based on several profiles to which we assigned the same error. A larger error (3 mm/yr) was assigned the *McGregor et al.* [1977] rate because the survey coverage ended just beyond the young edge of 2′ on the east side. A 4 mm/yr error was assigned to the *Vogt et al.* [1980] rates because no supporting data were given for these rates, which were taken from the rate-age plot.

Transform azimuths. The azimuths of transform faults were estimated from conventional bathymetric, Sea Beam, and Gloria data. We used several criteria for choosing transform data and estimating their errors. For the northern and southern segment of the Charlie-Gibbs transform fault we determined fault azimuths from the pole that is the center of the small circle that best fit each transform trace [*Searle*, 1981]. For three of the four Africa-North America transforms, we relied on the azimuth quoted by *Roest et al.* [1984]. For the Kane transform fault, we measured the azimuth from Pockalny et al. [1988]. For the Gloria fault, we found azimuths at several points, 3 taken directly from *Laughton et al.* [1972], and one from the location of Gloria lineaments near the east end of the fault [*Laughton and Whitmarsh*, 1974; *Searle*, 1979]. For the three transforms we found from conventional bathymetry [*Perry et al.*, 1978], we took latitude and longitude coordinates of the ridge-transform intersections from the bathymetric map and calculated the azimuths.

Errors were assigned to transform trends from subjective estimates of the accuracy of the data. Errors ranged from 2 to 10°, the most common error assigned being 3°. Errors for transform azimuths determined from precision-depth-recorder bathymetry ranged from 3 to 10°, depending on the linearity of the transform valley, the steepness of its slopes, and the accuracy with which the ridge-transform intersection was located. Azimuths along the Mid-Atlantic Ridge determined from Gloria surveys were given small errors of 2–3°, the exact value depending on the strength, width, and continuity of the imaged reflectors, the length of the transform fault, and the width of the principal transform displacement zone or transform fault zone. We think these small errors are realistic. Kane transform has been surveyed by both Gloria and Sea Beam, and the azimuths agree within 1°. For the total weight given to the Gloria fault system not to be several times greater than other Gloria-surveyed transform faults, we assigned large errors, 3–7°, to the four Gloria fault azimuths.

Slip vectors. Slip vectors were taken from several sources (Table 1) analyzing earthquakes that lie along transforms offsetting the Mid-Atlantic and Arctic ridges, and six earthquakes along the Azores-Gibraltar Ridge. We excluded slip vectors from the Tjornes transform fault (within the Iceland Platform) [*Saemundsson*, 1974; *Einarsson*, 1979] because its zone of seismicity is wide (80 km) and because it lacks a clear bathymetric expression. We also omitted slip vectors across continent-continent boundaries, such as in northeast Asia and the Mediterranean. The body-wave magnitudes of mechanisms from *Engeln et al.* [1986], *Cook et al.* [1986], *Bergman and Solomon* [1988], and *Grimison and Chen* [1986, 1988] exceed 5. Focal mechanisms of the largest earthquakes (M_S=5.8–6.9), which were determined by *Bergman and Solomon* [1988] using waveform inversion [*Nabelek*, 1984], were assigned 10° errors. We used 10 mechanisms showing slip on transform faults from the Harvard centroid moment tensor solutions published through June 1987. Errors of 10, 15, or 20° were assigned to these, depending on whether the earthquake had M_0 greater than 10^{25} dyn cm, M_0 between 10^{24} and 10^{25} dyn cm, or M_0 less than 10^{24} dyn cm, respectively. Mechanisms of intermediate-size earthquakes (five of six with m_b in the range 5.6–6.0) determined with older techniques and compiled by *Cook et al.* [1986] were assigned errors of 20°. Mechanisms of the smallest earthquakes (three of four with M_S between 5.2 and 5.5) from *Engeln et al.* [1986] were also given errors of 20°. An exception to these guidelines was made for slip vectors along the eastern Azores-Gibraltar Ridge, which despite being determined using waveform inversion were assigned larger errors of 25° because they are highly scattered and because of their ambiguous tectonic setting.

Middle Tier: Euler Vectors and Consistency of Data From a Single-Plate Boundary

We determine best fitting Euler vectors with a weighted least squares algorithm based on *Chase's* [1972] fitting functions. The functions are linear in rate but nonlinear in azimuth. We linearize the fitting functions about a trial solution and solve for parameter increments iteratively until the solution converges. Chase's formulation for rates fits the projection of the surface velocity vector onto the horizontal ridge-normal direction; thus observed rates must be ridge-normal, and the strike of the magnetic lineations, which we determined from the strike of anomaly 2′, must be specified. This differs from *Minster and Jordan's* [1978] analysis where observed rates are measured parallel to an assumed direction of relative motion. Here, neither approach offers an important advantage over the other, except that our program based on Chase's formulation runs 6 to 8 times faster than our program based on Minster and Jordan's formulation.

Euler vector confidence limits are determined by linear propagation of errors. To compare the standard error ellipse determined by *Minster and Jordan* [1978] with those given here, Minster and Jordan's errors must be multiplied by $2^{1/2}$ because they describe one-dimensional standard errors, whereas our standard errors are appropriate for two dimensions [cf. *Cox and Gordon*, 1984, Figures 3 and 4]. Values quoted or shown here for confidence limits from the prior studies of *Chase* [1978] and *Minster and Jordan* [1978] have been recomputed using our conventions, so that the new and old results are comparable.

To test the internal consistency of data from each individual plate boundary, we applied a statistical test for additional plate boundaries [*Stein and Gordon*, 1984], which is useful for locating plate boundaries poorly defined by seismicity and bathymetry, or for identifying systematic data biases. The test assumes that data from a boundary should be fit well by a single Euler vector if

both plates are rigid. If the same data are split at many hypothetical locations along the boundary, and each portion is fit by a different Euler vector, the misfit decreases. We use an F ratio test to determine whether the decrease is significantly greater than expected solely from introducing more adjustable parameters. An F value exceeding that expected at the 1% risk level suggests that an additional plate boundary intersects the boundary being analyzed, or that some of the data have systematic errors.

Upper Tier: Three-Plate Model and Plate Circuit Closure

We determine a three-plate model that enforces plate circuit closure using standard extensions of Euler vector determination for a single plate pair. Methods of inverting the data from three or more plate boundaries have been described before by *Chase* [1972] and *Minster et al.* [1974]. For any three plates, plate circuit closure permits any one Euler vector, here the Africa-Eurasia vector, to be predicted from the sum of the other two, here the Africa-North America and North America-Eurasia Euler vectors. In this paper we assess triple junction closure with two quantitative methods. In one, the best fitting Africa-Eurasia Euler pole is compared with a predicted vector, determined by summing the Africa-North America and Eurasia-North America best fitting Euler vectors. Confidence limits on the predicted vector are determined by linear propagation of errors.

We also assess triple junction closure with an F ratio test of plate circuit closure, which focuses on the differences in the overall fit of two different models to the data [*Gordon et al.*, 1987]. One model consists of three Euler vectors found by fitting all data while enforcing closure. Only six independent parameters are determined from the data. The second model consists of two Euler vectors and one Euler pole (for the Eurasia-Africa boundary along which no rate data are available) derived by fitting the data along each plate boundary separately. Because closure is unenforced, eight independent parameters are determined.

The test is formulated using χ^2, the total, weighted least squares misfit, and is analogous to the test of additional terms widely used in curve fitting. The χ^2 determined with eight adjustable parameters (N–8 degrees of freedom) is always less than the χ^2 determined from the same data but with only six adjustable parameters (N–6 degrees of freedom). To test if the reduction in χ^2 is greater than would be expected merely because more model parameters were added, the statistic

$$F_{2,N-8} = \frac{\left[\chi^2(6) - \chi^2(8)\right] / 2}{\chi^2(8) / (N-8)} \quad (1)$$

is used. This statistic is expected to be F distributed with 2 versus N–8 degrees of freedom [*Bevington*, 1969]. The experimentally determined value of F is compared with a reference value from tables [e.g., *Spiegel*, 1975] of $F_{2,N-8}$ with less than a 1% probability of being exceeded by chance. If the experimental value exceeds the reference value, then there is a 99% probability that closure is violated.

Acknowledgments. We thank Roger Searle and Sean Solomon for careful reviews, Peter Vogt for helpful discussions, and W.-P. Chen for a preprint. This work was supported by NSF grant 8721306, NASA Crustal Dynamics grant NAG5-885, and by an Alfred P. Sloan Foundation Research Fellowship (RGG).

REFERENCES

Allen, C. R., The modern San Andreas Fault, in *The Geotectonic Development of California, Rubey Vol. I*, edited by W. G. Ernst, pp. 511–534, Prentice-Hall, Englewood Cliffs, N. J., 1981.

Bergman, E. A., and S. C. Solomon, Transform fault earthquakes in the North Atlantic: Source mechanisms and depth of faulting, *J. Geophys. Res., 93*, 9027–9057, 1988.

Bevington, P. R., *Data Reduction and Error Analysis for the Physical Sciences*, McGraw-Hill, New York, 1969.

Bowen, A. N., and R. S. White, Deep-tow seismic profiles from the Vema transform and ridge-transform intersection, *J. Geol. Soc. London, 143*, 807–818, 1986.

Bungum, H., B. J. Mitchell, and Y. Kristoffersen, Concentrated earthquake zones in Svalbard, *Tectonophysics, 82*, 175–188, 1982.

Chapman, M. E., and S. C. Solomon, North America-Eurasian plate boundary in northeast Asia, *J. Geophys. Res., 81*, 921–930, 1976.

Chase, C. G., The N plate problem of plate tectonics, *Geophys. J. R. Astron. Soc., 29*, 117–122, 1972.

Chase, C. G., Plate kinematics: The Americas, East Africa, and the rest of the world, *Earth Planet. Sci. Lett., 37*, 355–368, 1978.

Collette, B. J., A. P. Slootweg, and W. Twigt, Mid-Atlantic ridge crest topography between 12° and 15°N, *Earth Planet. Sci. Lett., 42*, 103–108, 1979.

Cook, D. B., K. Fujita, and C. A. McMullen, Present-day plate interactions in northeast Asia: North American, Eurasian, and Okhotsk plates, *J. Geodyn., 6*, 33–51, 1986.

Cox, A., and R. G. Gordon, Paleolatitudes determined from paleomagnetic data from vertical cores, *Rev. Geophys., 22*, 47–72, 1984.

DeMets, C., R. G. Gordon, S. Stein, D. F. Argus, J. Engeln, P. Lundgren, D. G. Quible, C. Stein, S. A. Weinstein, D. A. Wiens, and D. F. Woods, NUVEL-1: A new global plate motion dataset and model (abstract), *Eos Trans. AGU, 66*, 368–369, 1985.

DeMets, C., R. G. Gordon, and D. Argus, Intraplate deformation and closure of the Australia-Antarctica-Africa plate circuit, *J. Geophys. Res., 93*, 877–897, 1988.

Dziewonski, A. M., A. Friedman, D. Giardini, and J. H. Woodhouse, Global seismicity of 1982: Centroid-moment tensor solutions for 308 earthquakes, *Phys. Earth Planet. Inter., 33*, 76–90, 1983.

Dziewonski, A. M., J. E. Franzen, and J. H. Woodhouse, Centroid-moment tensor solutions for April-June 1984, *Phys. Earth Planet. Inter., 37*, 87–96, 1985*a*.

Dziewonski, A. M., J. E. Franzen, and J. H. Woodhouse, Centroid-moment tensor solutions for July-September 1984, *Phys. Earth Planet. Inter., 38*, 203–213, 1985*b*.

Dziewonski, A. M., J. E. Franzen, and J. H. Woodhouse, Centroid-moment tensor solutions for April-June 1985, *Phys. Earth Planet. Inter., 41*, 215–224, 1986.

Dziewonski, A. M., G. Ekstrom, J. E. Franzen, and J. H. Woodhouse, Global seismicity of 1977: Centroid-moment tensor solutions for 471 earthquakes, *Phys. Earth Planet. Inter., 45*, 11–36, 1987*a*.

Dziewonski, A. M., G. Ekstrom, J. H. Woodhouse, and G. Zwart, Centroid-moment tensor solutions for October-December 1986, *Phys. Earth Planet. Inter., 48*, 5–17, 1987*b*.

Dziewonski, A. M., G. Ekstrom, J. E. Franzen, and J. H. Woodhouse, Global seismicity of 1979: Centroid-moment tensor solutions for 524 earthquakes, *Phys. Earth Planet. Inter., 48*, 18–47, 1987*c*.

Dziewonski, A. M., G. Ekstrom, J. E. Franzen, and J. H. Woodhouse, Global seismicity of 1980: Centroid-moment tensor solutions for 515 earthquakes, *Phys. Earth Planet. Inter., 50*, 127–154, 1988*a*.

Dziewonski, A. M., G. Ekstrom, J. E. Franzen, and J. H. Woodhouse, Global seismicity of 1981: Centroid-moment tensor

solutions for 542 earthquakes, *Phys. Earth Planet. Inter., 50,* 155–182, 1988*b*.
Einarsson, P., Seismicity and earthquake focal mechanisms along the mid-Atlantic plate boundary between Iceland and the Azores, *Tectonophysics, 55,* 127–153, 1979.
Eittreim, S., and J. Ewing, Vema Fracture Zone transform fault, *Geology, 3,* 555–558, 1975.
Engeln, J. F., D. A. Wiens, and S. Stein, Mechanisms and depths of Atlantic transform earthquakes, *J. Geophys. Res., 91,* 548–577, 1986.
Feden, R. H., P. R. Vogt, and H. S. Fleming, Magnetic and bathymetric evidence for the "Yermak Hot Spot" northwest of Svalbard in the Arctic Basin, *Earth Planet. Sci. Lett., 44,* 18–38, 1979.
Gordon, R. G., S. Stein, C. DeMets, and D. F. Argus, Statistical tests for closure of plate motion circuits, *Geophys. Res. Lett., 14,* 587–590, 1987.
Grimison, N. L., and W.-P. Chen, The Azores-Gibraltar plate boundary: Focal mechanisms, depths of earthquakes, and their tectonic implications, *J. Geophys. Res., 91,* 2029–2047, 1986.
Grimison, N. L., and W.-P. Chen, Source mechanisms of four recent earthquakes along the Azores-Gibraltar plate boundary, *Geophys. J. R. Astron. Soc., 92,* 391–401, 1988.
Harland, W. B., A. V. Cox, P. G. Llewellyn, C. A. G. Pickton, A. G. Smith, and R. Walters, *A Geologic Time Scale,* 131 pp., Cambridge University Press, New York, 1982.
Hirn, A., H. Haessler, P. H. Trong, G. Witlinger, and L. A. M. Victor, Aftershock sequence of the January 1st, 1980, earthquake and present-day tectonics in the Azores, *Geophys. Res. Lett., 7,* 501–504, 1980.
Karasik, A. M., Yevraziskii bassein cevernogo ledovitogo okeana s pozitsic tektonikz plit, *Problemi Geologic Polyarnikh Oblasteczeml,* pp. 24–31, NIDRA (in Russian), Leningrad 1974.
Klitgord, K. D., and H. Schouten, Plate kinematics of the Central Atlantic, in *The Geology of North America,* Vol. M, *The Western North Atlantic Region,* edited by P. R. Vogt and B. E. Tucholke, 351–378, Geological Society of America, Boulder, Colo., 1986.
Kovacs, L. C., C. Bernero, G. L. Johnson, R. H. Pilger, P. T. Taylor, and P. R. Vogt, *Residual Magnetic Anomaly Chart of the Arctic Ocean Region,* Naval Research Laboratory and Naval Ocean Research and Development Activity, Miss., 1982.
Laughton, A. S., and R. B. Whitmarsh, The Azores-Gibraltar plate boundary, in *Geodynamics of Iceland and the North Atlantic Area,* edited by L. Kristjansson, pp. 63–81, D. Reidel, Hingham, Mass., 1974.
Laughton, A. S., R. B. Whitmarsh, J. S. M. Rusby, M. L. Somers, J. Revie, and B. S. McCartney, A continuous east-west fault on the Azores-Gibraltar Ridge, *Nature, 327,* 217–220, 1972.
Le Douaran, S., H. D. Needham, and J. Francheteau, Pattern of opening rates along the axis of the Mid-Atlantic Ridge, *Nature, 300,* 254–257, 1982.
Lynnes, C. S., and L. J. Ruff, Source process and tectonic implications of the great 1975 North Atlantic earthquake, *Geophys. J. R. Astron. Soc., 82,* 497–510, 1985.
Macdonald, K. C., Near-bottom magnetic anomalies, asymmetric spreading, oblique spreading and tectonics of the Mid-Atlantic Ridge near Lat 37°N, *Geol. Soc. Am. Bull., 88,* 541–555, 1977.
Macdonald, K. C., The crest of the Mid-Atlantic Ridge: Models for crustal generation processes and tectonics, in *The Geology of North America,* Vol. M, *The Western North Atlantic Region,* edited by P. R. Vogt and B. E. Tucholke, 51–68, The Geological Society of America, Boulder, Colo., 1986.
Macdonald, K. C., and B. P. Luyendyk, Deep-tow studies of the structure of the Mid-Atlantic Ridge crest near Lat 37°N, *Geol. Soc. Am. Bull., 88,* 621–636, 1977.
Macdonald, K. C., D. Castillo, S. Miller, P. J. Fox, K. Kastens, and E. Bonatti, Deep-tow studies of the Vema fracture zone, 1, Tectonics of a major slow slipping transform fault and its intersection with the Mid-Atlantic ridge, *J. Geophys. Res., 91,* 3334–3354, 1986.
McGregor, B. A., C. G. A. Harrison, J. W. Lavelle, and P. A. Rona, Magnetic anomaly patterns on Mid-Atlantic ridge crest at 26°N, *J. Geophys. Res., 82,* 231–238, 1977.
McKenzie, D. P., Active tectonics of the Mediterranean region, *Geophys. J. R. Astron. Soc., 30,* 109–185, 1972.
Minster, J. B., and T. H. Jordan, Present-day plate motions, *J. Geophys. Res., 83,* 5331–5354, 1978.
Minster, J. B., T. H. Jordan, P. Molnar, and E. Haines, Numerical modeling of instantaneous plate tectonics, *Geophys. J. R. Astron. Soc., 36,* 541–576, 1974.
Morgan, W. J., Rises, trenches, great faults, and crustal blocks, *J. Geophys. Res., 73,* 1959–1982, 1968.
Nabelek, J. L., Determination of earthquake source parameters from inversion of body waves, Ph.D. dissertation, Mass. Inst. of Technol., Cambridge, 1984.
Parson, L. M., and R. C. Searle, Strike-slip fault styles in slow-slipping oceanic transform faults—Evidence from GLORIA surveys of Atlantis and Romanche Fracture Zones, *J. Geol. Soc. London, 143,* 757–761, 1986.
Perry, R. K., H. S. Fleming, N. Z. Cherkis, R. H. Feden, and P. R. Vogt, *Bathymetry of the Norwegian-Greenland and Western Barents Seas,* Naval Research Laboratory, Acoustics Division, Washington, D.C., 1978.
Pockalny, R. A., R. S. Detrick, and P. J. Fox, The morphology and tectonics of the Kane Transform from Sea Beam bathymetry data, *J. Geophys. Res., 93,* 3179–3193, 1988.
Purdy, G. M., P. D. Rabinowitz, and H. Schouten, The Mid-Atlantic Ridge at 23°N: Bathymetry and magnetics, *Initial Rep. Deep Sea Drill. Proj., 45,* 119–128, 1979.
Rabinowitz, P. D., and H. Schouten (Eds.), *Mid-Atlantic Ridge Between 22° and 38°N, Atlas 11, Ocean Margin Drilling Program, Regional Atlas Ser.,* Marine Science International, Woods Hole, Mass., 1985.
Roest, W. R., Seafloor spreading pattern of the North Atlantic between 10° and 40°N, Ph.D. dissertation, 121 pp., Univ. of Utrecht, 1987.
Roest, W. R., R. C. Searle, and B. J. Collette, Fanning of fracture zones and a three-dimensional model of the Mid-Atlantic Ridge, *Nature, 308,* 527–531, 1984.
Rona, P. A., and D. F. Gray, Structural behavior of fracture zones symmetric and asymmetric about a spreading axis: Mid-Atlantic Ridge (latitude 23°N to 27°N), *Geol. Soc. Am. Bull., 91,* 485–494, 1980.
Ruegg, J. C., M. Kasser, A. Tarantola, J. C. Lepine, and B. Chouikrat, Deformations associated with the El Asnam earthquake of 10 October 1980: Geodetic determination of vertical and horizontal movements, *Bull. Seismol. Soc. Am., 72,* 2227–2244, 1982.
Saemundsson, K., Evolution of the axial rifting zone in northern Iceland and the Tjornes Fracture Zone, *Geol. Soc. Am. Bull., 85,* 495–504, 1974.
Savostin, L. A., and A. M. Karasik, Recent plate tectonics of the Arctic Basin and of northeastern Asia, *Tectonophysics, 74,* 111–145, 1981.
Schouten, H., and K. McCamy, Filtering marine magnetic anomalies, *J. Geophys. Res., 77,* 7089–7099, 1972.
Searle, R. C., Side-scan studies of North Atlantic fracture zones, *J. Geol. Soc. London, 136,* 283–292, 1979.
Searle, R., Tectonic pattern of the Azores spreading centre and triple junction, *Earth Planet. Sci. Lett., 51,* 415–434, 1980.
Searle, R., The active part of Charlie-Gibbs Fracture Zone: A study using sonar and other geophysical techniques, *J. Geophys. Res., 86,* 243–262, 1981.
Searle, R. C., GLORIA investigations of oceanic fracture zones: Comparative study of the transform fault zone, *J. Geol. Soc. London, 143,* 743–756, 1986.
Searle, R. C., and A. S. Laughton, Sonar studies of the Mid-Atlantic Ridge and Kurchatov Fracture Zone, *J. Geophys. Res., 82,* 5313–5328, 1977.
Spiegel, M. R., *Schaum's Outline of Theory and Problems of Probability and Statistics,* 372 pp., McGraw-Hill, New York, 1975.
Srivastava, S. P., and C. R. Tapscott, Plate kinematics of the North Atlantic, in *The Geology of North America,* Vol. M, *The Western North Atlantic Region,* edited by P. R. Vogt and B. E. Tucholke, 379–404, Geological Society of America, Boulder, Colo., 1986.
Stein, S., and R. G. Gordon, Statistical tests of additional plate

boundaries from plate motion inversions, *Earth Planet. Sci. Lett., 69,* 401–412, 1984.

Talwani, M., C. C. Windisch, and M. G. Langseth, Reykjanes ridge crest: A detailed geophysical study, *J. Geophys. Res., 76,* 473–517, 1971.

Udias, A., A. L. Arroyo, and J. Mezcua, Seismotectonics of the Azores-Alboran region, *Tectonophysics, 31,* 259–289, 1976.

Vogt, P. R., P. T. Taylor, L. C. Kovacs, and G. L. Johnson, Detailed aeromagnetic investigation of the Arctic Basin, *J. Geophys. Res., 84,* 1071–1089, 1979.

Vogt, P. R., G. L. Johnson, and L. Kristjansson, Morphology and magnetics anomalies north of Iceland, *J. Geol., 47,* 67–80, 1980.

Vogt, P. R., L. C. Kovacs, C. Bernero, and S. P. Srivastava, Asymmetric geophysical signatures in the Greenland-Norwegian and southern Labrador seas and the Eurasian Basin, *Tectonophysics, 89,* 95–160, 1982.

Yielding, G., Control of rupture by fault geometry during the 1980 El Asnam (Algeria) earthquake, *Geophys. J. R. Astron. Soc., 81,* 641–670, 1985.

D. F. Argus, R. G. Gordon, and S. Stein, Department of Geological Sciences, Northwestern University, Evanston, IL 60208.

C. DeMets, Naval Research Laboratory, Code 5110, Washington, DC 20375.

(Received February 2, 1988;
revised October 24,, 1988;
accepted May 2, 1988.)